Molecular modeling of N,N-disubstituted hydrazine phosphorus-containing dendrimers of the fourth generation

Ahmed Ibrahim Abou-Kandil, Wolfgang Knoll

Molecular Simulation
Journal of
Experimental Nanoscience

Taylor & Francis
Taylor & Francis Group

Molecular modeling of N,N-disubstituted hydrazine phosphorus-containing dendrimers of the fourth generation

Journal:	*Molecular Simulation/Journal of Experimental Nanoscience*
Manuscript ID:	GMOS-2007-0154.R1
Journal:	Molecular Simulation
Date Submitted by the Author:	28-Jan-2008
Complete List of Authors:	Abou-Kandil, Ahmed; Max-Planck Institute for Polymer Research, Materials Science Knoll, Wolfgang; Max-Planck Institute for Polymer Research, Materials Science
Keywords:	dendrimers, molecular simulation, amorphous cell

Molecular modeling of N,N-disubstituted hydrazine phosphorus-containing dendrimers of the fourth generation

Ahmed I. Abou-Kandil* and Wolfgang Knoll

Max-Planck Institute for Polymer Research. Ackermannweg 10. Mainz. 55128. Germany

Abstract

Dendritic polymers are regarded as highly branched regular three-dimensional monodisperse macromolecules with a branch occurring at each monomer unit. Our present study looks into more details in the molecular structure of globular N,N-disubstituted hydrazine phosphorus-containing dendrimers of the fourth generation having 96 terminal groups with either cationic $[G_4(NH^+Et_2Cl^-)_{96}]$ (G_4^+) or anionic $[G_4(CHCOO^-Na^+)_{96}]$ (G_4^-) character. We show that the behavior of those dendrimers in water leads to the formation of a branched, star-like structure, yet this structure is not completely spherical as previously thought of. The importance of this finding can explain the differences in thickness of dendrimer thin films produced by Layer-By-Layer deposition. The dendrimers were built, their behavior in water and energy minimization of the system were carried out using computing routines contained within the *Materials Studio* software.

Introduction

Dendritic polymers, referred mostly as dendrimers are highly branched regular three-dimensional monodisperse macromolecules with a branch occurring at each monomer unit. Large dendrimers adopt a globular shape. They are characterized by the presence of a large number of functional groups on the surface which results in solubility, viscosity, and thermal behaviors different from those of more classical polymers. They are also

* Corresponding Author: aia_23@yahoo.co.uk

characterized by the presence of internal cavities which can be functionalized and by a core that does or does not bear functional groups. There are several dendrimers prepared in many different synthetic routs order to achieve certain electronic and/or magnetic properties **[1-8]**. The general structure of those dendrimers can be schematically represented in figure (1).

The increase in the number of branches and the variety of the core structure also controls the architecture of these dendrimers; not only affecting the chemical properties but also the physical properties too in terms of rigidity of the overall structure and/or its ability to interact with an electric or magnetic fields.

Several types of dendrimers generations 2, 3 and 4 have been synthesized especially to carry either a positive or negative charges on their outer surface finding applications in layer-by-layer assembly of supramolecular structures **[9-14]**.

The alternate deposition of G_4^-/G_4^+ by the Layer-by-Layer (LbL) deposition was successfully demonstrated and has shown a monotonous increase in film thickness as a function of the number of bilayers. The composite multilayers comprised of these shape persistent dendrimers and nanocrystals could be utilized as nanostructured building blocks with excellent control over their porosity, functionality, and dimension **[13,14]**.

The multilayers comprised of pure dendrimers were characterized by electrochemistry to examine the permeability properties using $[Fe(CN)_6]^{3-/4-}$ as the redox couple. All the previous experimental studies did not touch the modeling of such massive dendritic polymers and/or elaborate their behavior in water which is crucial to the LBL deposition either or flat Gold surface and/or functionalized Alumina surfaces.

Previous modeling studies done on dendrimers showed that charged and uncharged Poly (amidoamine), PAMAM, dendrimers strongly adsorb to mica surfaces resulting in deformation of the molecules **[16]**. Modeling of other dendrimer structures show hydrogen bonding upon aggregation although in the minimum energy conformation such

hydrogen bonds did not exist **[17]**. Modeling also helped assigning proton and carbon resonances of first- and second-generation phenol-terminated carbosilane dendrimers and the second generation of the analogous titanium-ended carbosilane dendrimer **[18]** and to reveal the structure stilbenoid dendrimers of third generation by the help of small angle x-ray scattering **[19]**. The use of unsymmetrical dendrimers was demonstrated to provide nanoscale platforms for design of bimolecular guest binding receptors **[20]** and a promising vehicle for intracellular delivery of low-solubility drugs **[21]**.

Several modeling studies of dendritic polymers dealt with self assembly of those polymers **[22-27]** or the properties and applications of different dendrimers in biological and pharmaceutical applications **[28-32]**.

Our present study looks into more details in the molecular structure of globular N,N-disubstituted hydrazine phosphorus-containing dendrimers of the fourth generation having 96 terminal groups with either cationic $[G_4(NH^+Et_2Cl^-)_{96}]$ (G_4^+) or anionic $[G_4(CHCOO^-Na^+)_{96}]$ (G_4^-) character. The chemical structure of both dendrimers is illustrated in figure (2).

Results and molecular modeling procedure

Materials Studio® software provided by *Accelrys*® has been used to model the structure of such a massive dendrimer. Other software provided by the same company has been used successfully in modeling the intermediate smectic mesophase in polyethylene terephthalate **[33]**. The software has also been used to model inclusion of drugs **[34]**, drug delivery **[35]**, calculation of radius of gyration of dendrimers **[36,37]** and calculating properties of supramolecular structures **[38,39]**.

1- The *builder* in *Materials Studio* was used to build the G_4^+ and G_4^- dendrimers under investigation. The seed structure was built separately in a 3D atomistic document. The correct number of generations is constructed using the building fragments in order to build the G_4 dendrimers. Connection points were clearly

indicated on the dendrimer seed and fragment. The new dendrimers were then created and viewed in 3D atomistic document.

2- Finally the terminating fragment was built carrying either carboxylic acid or a tertiary amide group and connected to the building fragments in order to create the correct structure of the dendrimer carrying either 96 negative or positive charges respectively.

3- The structure resulting from initial dendrimers were *"cleaned"* to tidy up the geometry. This is not an energy minimization, but, instead, uses a look-up table of standard bond lengths and angles to give a first approximation to the correct geometry of the modeled dendrimers.

The structure of the seed, building fragment, positive and negative termination fragments as well as the over all structure of the positively and negatively charged dendrimers are illustrated in figure (3). We emphasize here the planar structure of the planar structure of the N_3P_3 core, figure 3A, as well as the N-P bond in the Building fragment, figure 3-B.

4- In order to add water to the system, an *"amorphous cell"* is constructed where one dendrimer (to reduce the simulation time) is added in a confined space with a certain number of water molecules. The number of water molecules used in the simulations discussed here ranged between 1000 and 2000 water molecules. This helped in reducing the computation time limiting the total number of atoms contained in the system ~ 10,000.

5- Amorphous cells were constructed so that the end density of the resulting cell is 1. This was done by adjusting the cell dimensions and the number of water molecules. Adjusting the density value corresponds to the actual density values obtained experimentally at concentrations of 1 mg ml^{-1}**[14]**.

The resulting amorphous cell containing both the positively and negatively charged dendrimers are shown in figure (4).

6- The energy of the resulting amorphous cell was minimized using the *smart minimizer*. This method combines the following steps:

a- *Steepest Descent*, quickly reduces energy, this step is composed mainly of the so-called *line search*, which modifies the coordinates to generate a new, lower-energy structure. The line search direction is defined along the direction of the local downhill gradient. It will quickly reduce the energy of the structure during the first few iterations. However, convergence will slow down considerably as the gradient approaches zero. It is used when the gradients are very large and the configurations are far from the minimum; typically for poorly refined crystallographic data, or for graphically built molecules **[40]**.

b- *Conjugate Gradient*, compares energy with previous iteration, this improves the line search direction by storing information from the previous iteration. It is chosen because the system is too large for storing and manipulating a second-derivative matrix. The time per iteration is longer than for steepest descents, but this is more than compensated for by efficient convergence **[41,42]**.

c- *Newton-Rhaphson,* when the system is close to zero potential. It requires computation and storage of second derivatives and thus expensive in terms of computer resources. For this reason it is only recommended for systems with a maximum of 200 atoms. However, it has a small convergence radius but it is very efficient near the energy minimum **[43]**.

7- Applying all previous three steps in a cascading manner adding to that the equilibrium values of bond lengths and angles, plus the force constants, Van-der-

Waals radii and associated constants required to calculate the nonbonded interactions.

Discussion

The combination of all previous parameters with the functional forms of the individual energy terms is known as a forcefield. COMPASS (Condensed-Phase Optimized Molecular Potentials for Atomistic Simulation Studies) is the forcefield used in the energy minimization in the present report. It is an *ab-initio* based forcefield that was parameterized using extensive data for molecules in the condensed phase. It is able to make accurate predictions of structural, conformational, and vibrational, properties for a broad range of compounds, especially polymers, both in isolation and in condensed phases **[33-36,38,39]**.

The coordinates of a structure combined with the COMPASS forcefield create an *energy expression*. This energy expression is the equation that describes the potential energy surface of a particular structure as a function of its atomic coordinates.

The potential energy in this case can be expressed as a sum of valence (or bond), cross term and non-bond interactions as represented in equation {1}:

$$E_{total} = E_{valence} + E_{crossterm} + E_{non\text{-}bond} \qquad \{1\}$$

The energy of *valence* interactions is generally accounted for by bond stretching, valence angle bending, dihedral angle torsion and inversion, also called out-of-plane (oop) interactions terms, which are part of the forcefield for covalent systems and the Urey-Bradley (UB) term may be used to account for interactions between atom pairs involved in 1-3 configurations, i.e. atoms bound to a common atom. This is represented in equation {2}:

$$E_{valence} = E_{bond} + E_{angle} + E_{torsion} + E_{oop} + E_{UB} \qquad \{2\}$$

Cross terms are used to account for factors as bond or angle distortions caused by nearby atoms. These terms are required to accurately reproduce experimental vibrational frequencies and, therefore, the dynamic properties of molecules. Cross terms can include stretch-stretch, stretch-bend-stretch, bend-bend, torsion-stretch, torsion-bend-bend, bend-torsion-bend, and stretch-torsion-stretch. *Non-bond* interactions are accounted for by Van der Waals, electrostatic (Coulomb) and hydrogen bond terms, represented in equation {3}:

$$E_{non\text{-}bond} = E_{vdW} + E_{Coulomb} + E_{hbond} \qquad \{3\}$$

As an example for the complete energy expression, for water molecules we consider the following equation, {4}, which might be used to describes the potential energy surface of a water structure:

$$V(R) = K_{oh}\left(b - b_{oh}^{0}\right)^2 + K_{oh}\left(b' - b_{oh}^{0}\right)^2 + K_{hoh}\left(\theta - \theta_{hoh}^{0}\right)^2 \qquad \{4\}$$

The forcefield defines the bond lengths (b) and angles (q), the functional form (a simple quadratic in both types of coordinates, the force constants (K), the reference O-H bond length (b^0) and H-O-H angle (q^0) are the values for an ideal O-H bond and H-O-H angle at zero energy, which is not necessarily the same as their equilibrium values in a real water molecule.

The expression corresponding to the general, summed forcefield function can be written as follows in equation {5}:

$$\begin{aligned} V(R) = & \sum_{b} D_b \left[1 - \exp(-a(b - b_0))\right]^2 + \sum_{\theta} H_\theta (\theta - \theta_0)^2 + \sum_{\phi} H_\phi \left[1 + s\cos(n\phi)\right] \\ & + \sum_{\chi} H_\chi \chi^2 + \sum_{b}\sum_{b'} F_{bb'}(b - b_0)(b' - b'_0) + \sum_{\theta}\sum_{\theta'} F_{\theta\theta'}(\theta - \theta_0)(\theta' - \theta'_0) \\ & + \sum_{b}\sum_{\theta} F_{b\theta}(b - b_0)(\theta - \theta_0) + \sum_{\theta}\sum_{\theta'} F_{\theta\theta'\phi}(\theta - \theta_0)(\theta' - \theta'_0)\cos\phi \\ & + \sum_{\chi}\sum_{\chi'} F_{\chi\chi'}\chi\chi' + \sum_{i}\sum_{j>i}\left[\frac{A_{ij}}{r_{ij}^{12}} - \frac{B_{ij}}{r_{ij}^{6}} + \frac{q_i q_j}{r_{ij}}\right] \end{aligned} \qquad \{5\}$$

The first four terms in equation {5} are sums that reflect the energy needed to stretch bonds (b), bend angles (q) away from their reference values, rotate torsion angles (f) by twisting atoms about the bond axis that determines the torsion angle and distort planar atoms out of the plane formed by the atoms they are bonded to (c).

The next five terms in equation {5} are cross terms that account for interactions between the four types of internal coordinates.

The final term in equation {5} represents the non-bond interactions as a sum of repulsive and attractive Lennard-Jones terms as well as Coulombic terms, all of which are a function of the distance (r_{ij}) between atom pairs.

All these terms are included in the COMPASS forcefield were validated in earlier studies **[44-47]** and used in the accelrys software. More mathematical details are not shown here for simplicity but can be referred to on the *accelrys* website (www.accelrys.com) and in the help menu of *materials studio* and other related software e.g. *cerius*^{2}, it is also dealt with in more details during the validation studies of the forcefield **[44-47]**.

Values of bond lengths, bond angles, dihedral angles as well as exact co-ordinates of each atom are always saved in special file during energy minimization process. Initial values are consistent with those reported in the literature **[48-51]**. The resulting structure after energy minimization procedure explained above for the positively and negatively charged dendrimers are shown in figures (5) and (6). 5000 iterations were applied to minimize the energy. Only the scale of 200 iterations are shown in graphs (5-A) and (6-A) for clarity and simplicity purposes. This shows how the *steepest descent* method and the *conjugate gradient* method were used efficiently to reduce the potential energy of the amorphous cell to approach zero. The *Newton-Ralphson* method was used afterwards to refine the structure.

Conclusion

Materials Studio was used efficiently to build a dendrimer/water amorphous cell. It allowed us to minimize the energy of the resulting structure and study the actual behavior in water. This system is of extreme importance for bio-sensing and will be explored further in order to examine the behavior of the system in the presence of counter ions. The model obtained so far shows that these dendrimers under investigation are not completely spherical as they were first regarded. Also the long branches tend to bend giving the dendrimer a diameter of *ca* ~ 1-2 nm which is in good agreement with Surface Plasmon Resonance (SPR) experimental studies performed in our group **[13,14,52]**. We are in the process of not only validating experimental data using *materials studio* but of predicting the structures and their behavior to suit our experimental needs.

Acknowledgement

AIA would like to thank Drs. Alexandra Simperler and Carsten Menke from *accelrys* for their initial help with *materials studio* setup. Funding from the IDB during the period from January 2007 until December 2007 is greatly appreciated.

References

1- Nathalie Launay, Anne-Marie Caminade, Roger Lahana und Jean-Pierre Majoral, ***Angew. Chem.*** **1994,** 106. ***Nr.*** 15/16, 1682

2- Marcel Wesolek, Daniel Meyer, John A. Osborn, Andrk De Cian, Jean Fischer, Alain Derory, ***Angew. Chem. Int. Ed. Eng***. **1994,** 33. ***Nr.*** 15/16, 1529

3- Jean-Pierre Majoral and Anne-Marie Caminade, ***Chem. Rev***. **1999,** *99,* 845

4- Marie-Laure Lartigue, Michael Slany, Anne-Marie Caminade," and Jean-Pierre Majoral, ***Chem. Eur. J.*** **1996**, 2, 11, 1417.

5- Nathalie Launay, Michael Slany, Anne-Marie Caminade, and Jean Pierre Majoral, ***J. Org. Chem***. **1996,** *61,* 3799

6- Lucie Routaboul, Sandrine Vincendeau, Cedric-Olivier Turrin, Anne-Marie Caminade, Jean-Pierre Majoral, Jean-Claude Daran, Eric Manoury***, Journal of Organometallic Chemistry,*** **2007**, 692 1064.

7- Paul Servin, Cyrille Rebout, Regis Laurent, Maurizio Peruzzini, Anne-Marie Caminadea, and Jean-Pierre Majoral, ***Tetrahedron Letters***, **2007**, 48, 579

8- Laurent Brauge, Gilles Veriot, Gregory Franc, Rodolphe Deloncle, Anne-Marie Caminade, and Jean-Pierre Majoral, ***Tetrahedron***, **2006**, 62, 11891

9- Anne-Marie Caminade and Jean-Pierre Majoral, ***Accounts of Chemical Research,*** **2004,** 37 (6), 341

10- Dong Ha Kim, Jose Luis Hernandez-Lopez, Jianyun Liu, George Mihov, Linjie Zhi, Roland E. Bauer, Dorte Grebel-Kohler, Markus Klapper, Tanja Weil, Klaus Mullen, Silvia Mittler, Wolfgang Knoll, ***Macromol. Chem. Phys***. **2005**, 206, 52

11- Byoung-Suhk Kim, Olga V. Lebedeva, Dong Ha Kim, Anne-Marie Caminade, Jean-Pierre Majoral, Wolfgang Knoll, and Olga I. Vinogradova, ***Langmuir,*** **2005**, 21, (16), 7200

12- Z Liang, A S Susha, A Yu, F Caruso, **Advanced** ***Materials***, **2003**, 15 (21), 1849

13- Dong Ha Kim, Prabhu Karan, Petra Gçring, Julien Leclaire, Anne-Marie Caminade, Jean-Pierre Majoral, Ulrich Gçsele, Martin Steinhart, and Wolfgang Knoll, ***Small***, **2005**, 1 (1), 99

14- Chuan-Liang Feng, Xinhua Zhong, Martin Steinhart, Anne-Marie Caminade, Jean-Pierre Majoral, and Wolfgang Knoll, ***Adv. Mater.*** **2007**, *19*, 1933

15- S. Merino, L. Brauge, A. M. Caminade, J. P. Majoral, D. Taton, Y. Gnanou, ***Chem. Eur. J.*** **2001**, *7*, 3095.

16- A. Mecke, I. Lee, J.R. Baker jr., M.M. Banaszak Holl, and B.G. Orr, ***Eur. Phys. J. E***, **2004**, 14, 7

17- Z. Balogh, I. Palinko, ***Journal of Molecular Structure (Theochem)***, **2003**, 623, 11

18- Karen T. Welch, Silvia Arevalo, John F. C. Turner, and Rafael Gomez, ***Chem. Eur. J.*****, 2005**, 11, 1217

19- Sabine Rosenfeldt, Elena Karpuk, Matthias Lehmann, Herbert Meier, Peter Lindner, Ludger Harnau, and Matthias Ballauff, ***ChemPhysChem*****, 2006**, 7, 2097

20- Satoshi Shinoda, Masakazu Ohashi, and Hiroshi Tsukube, ***Chem. Eur. J.*** **2007**, 13, 81

21- Jayant J. Khandare, Sreeja Jayant, Ajay Singh, Pooja Chandna, Yang Wang, Nicholi Vorsa, and Tamara Minko, ***Bioconjugate Chem.,*** **2006,** 17, 1464

22- D. B. Amabilino, P. R. Ashton, V. Balzani, C. L. Brown, A. Credi, J. M. J. Frechet, J. W. Leon, F. M. Raymo, N. Spencer, J. F. Stoddart, and M. Venturi, ***J. Am. Chem. Soc.,*** **1996,** *118,* 12012

23- Diego J. Diaz, Gregory D. Storrier, Stefan Bernhard, Kazutake Takada, and Hector D. Abruna, ***Langmuir,*** **1999,** *15,* 7351

24- Diego J. Diaz, Stefan Bernhard, Gregory D. Storrier, and Hector D. Abruna, ***J. Phys. Chem. B,*** **2001,** *105,* 8746

25- S. Granick, S. K. Kumar, E. J. Amis, M. Antonietti, A. C. Balazs, A. K. Chakraborty, G. S. Grest, C. Hawker, P. Janmey, E. J. Kramer, R. Nuzzo, T. P. Russel, C. R. Safinya, ***Journal of Polymer Science: Part B: Polymer Physics***, **2003**, 41, 2755

26- Youngseon Choi, Almut Mecke, Bradford G. Orr, Mark M. Banaszak Holl, and James R. Baker, Jr., ***Nano Lett.,*** **2004**, 4 (3), 391

27- Izabela Bury, Beno.t Heinrich, Cyril Bourgogne, Daniel Guillon, and Bertrand Donnio, ***Chem. Eur. J.,*** **2006**, 12, 8396

28- S. Fomine, L. Fomina, P. Guadarrama, ***Macromol. Symp.,*** **2003**, 192, *43*

29- Ioannis Tsogas, Dimitris Tsiourvas, George Nounesis, and Constantinos M. Paleos, ***Langmuir,*** **2006,** *22,* 11322

30- T. J. Prosa, B. J. Bauer, E. J. Amis, D. A. Tomalia, R. Scherrenber, ***Journal of Polymer Science: Part B: Polymer Physics***, **1997**, 35, 2913

31- F. M. Menger, A. V. Peresypkin, S. Wu, ***J. Phys. Org. Chem.,*** **2001**, 14, 392

32- T. Cagin, G. Wang, R. Martin, G. Zamanakos, N. Vaidehi, D. T. Mainz, W. A. Goddard III, ***Computational and Theoretical polymer science*****, 2001**, 11, 345

33- Ahmed I. Abou-Kandil, Gerhard Goldbeck-Wood and Alan H. Windle, ***Macromolecules*****, 2007**, 40 (18), 6448

34- S. Pricl, M. Fermeglia, ***Carbohydrate Polymers*****, 2001**, 45, 23

35- Lorenzo Metullio, Marco Ferrone, Alessandro Coslanich, Sabine Fuchs, Maurizio Fermeglia, Maria Silvia Paneni, and Sabrina Pricl, ***Biomacromolecules*** **2004,** 5, 1371

36- Wilfredo Ortiz, Adrian E. Roitberg, and Jeffrey L. Krause, ***J. Phys. Chem. B*** **2004,** *108,* 8218

37- Sheng Zhang, Yannick Rio, Francüois Cardinali, Cyril Bourgogne, Jean-Louis Gallani, and Jean-Francüois Nierengarten, ***J. Org. Chem.,*** **2003**, *68*, 9787

38- Kailiang Yin, Dinghui Zou, Jing Zhong, Duanjun Xu, ***Computational Materials Science*****, 2007**, 38, 538

39- M. Grujicic, Y.-P. Sun, K.L. Koudela, ***Applied Surface Science***, **2007**, 253, 3009

40- M. Levitt, S. Lifson, ***J. Mol. Biol.***, **1969**, 46, 269

41- R. Fletcher, C. M. Reeves, ***Comput. J.***, **1964**, 7, 149

42- W.H. Press, B. P. Flannery, S.A. Teukolsky, W. T. Vetterling, ***Numerical Recipes, The Art of Scientific Computing***, Cambridge University Press, Cambridge, 1986.

43- O. Ermer, Calculation of molecular properties using force fields. Applications in organic chemistry, ***Struct. Bond.***, **1976**, 27, 161

44- H. Sun, ***J. Phys. Chem. B.***, **1998**, 338

45- H. Sun, D. Rigby, ***Spectrochimica Acta*** **A, 1997**, 53, 1301

46- D. Rigby, H. Sun, B. E. Eichinger, ***Polymer International***, **1997**, 44, 311

47- T. Spyriouni, C. Vergelati, ***Macromolecules***, **2001**, 34, 5306

48- M-L Lartigue, B Donnadieu, C Galliot, A-M Caminade and J-P Majoral, J-P Fayet. ***Macromolecules*, 1997**, 30, 7335

49- C Larre, B Donnadieu, A-M Caminade, and J-P Majoral, ***J. Am. Chem. Soc.*, 1998**, 120, 4029

50- C Larre, D Bressolles, C Turrin, B Dommadieu, A-M Caminade, and J-P Majoral, ***J. Am. Chem. Soc.*, 1998**, 120, 13070

51- V Maraval, R Laurent, B Donnadieu, M Mauzac, A-M Caminade, and J-P Majoral, ***J. Am. Chem. Soc.*, 2000**, 122, 2499

52- Ahmed I. Abou-Kandil and W. Knoll, *in preparation*

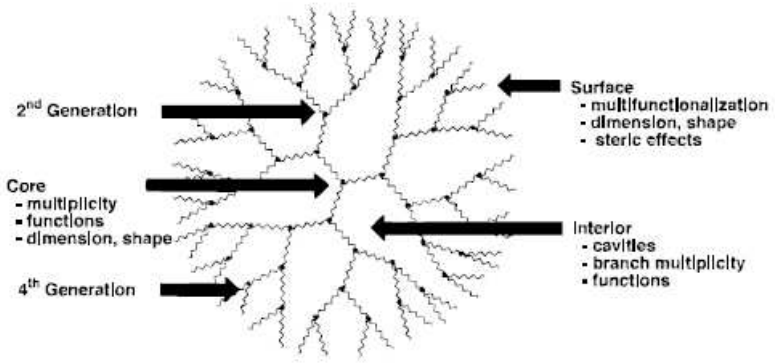

Figure (1): Schematic representation of a fourth generation dendrimer.

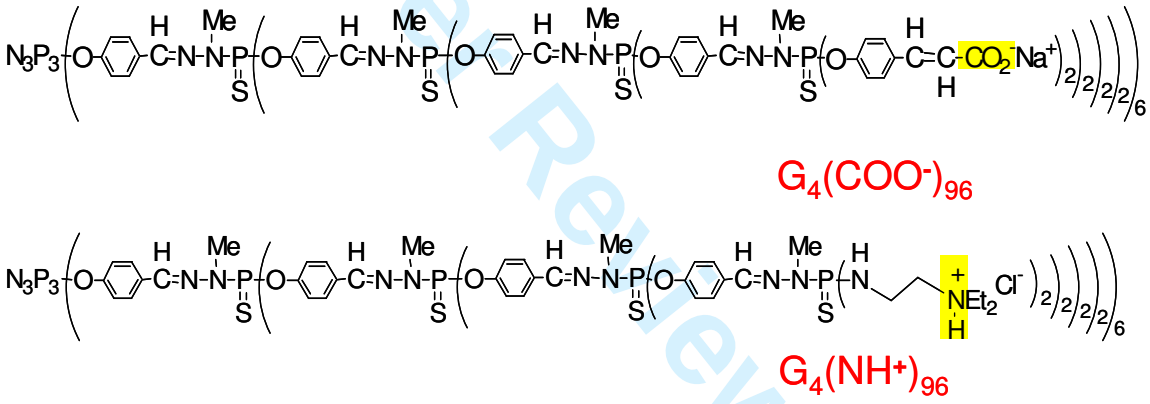

Figure (2): Chemical structure of the positively and negatively charged dendrimers.

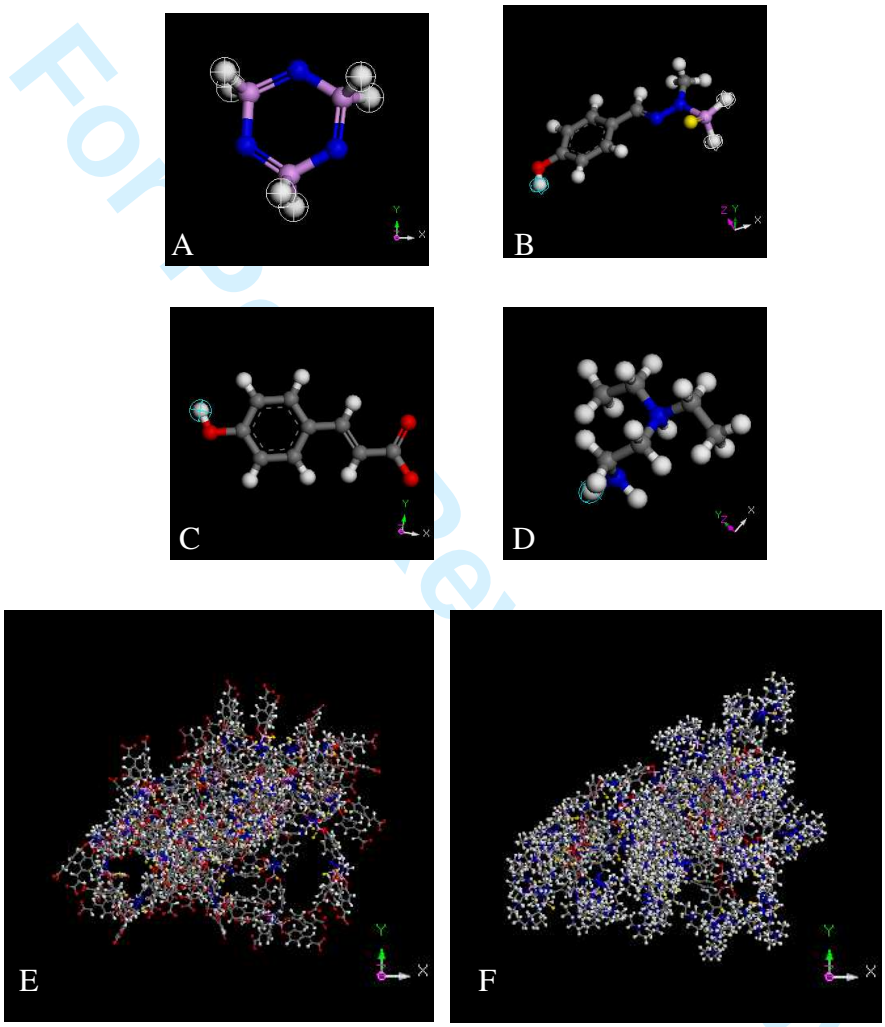

Figure (3): Structure of the (A): N_3P_3 Building core; (B); Building Fragment; (C): negatively charged terminating fragment; (D): positively charged terminating fragment; (E): negatively charged G_4 dendrimer; and (F): positively charged G_4 dendrimer

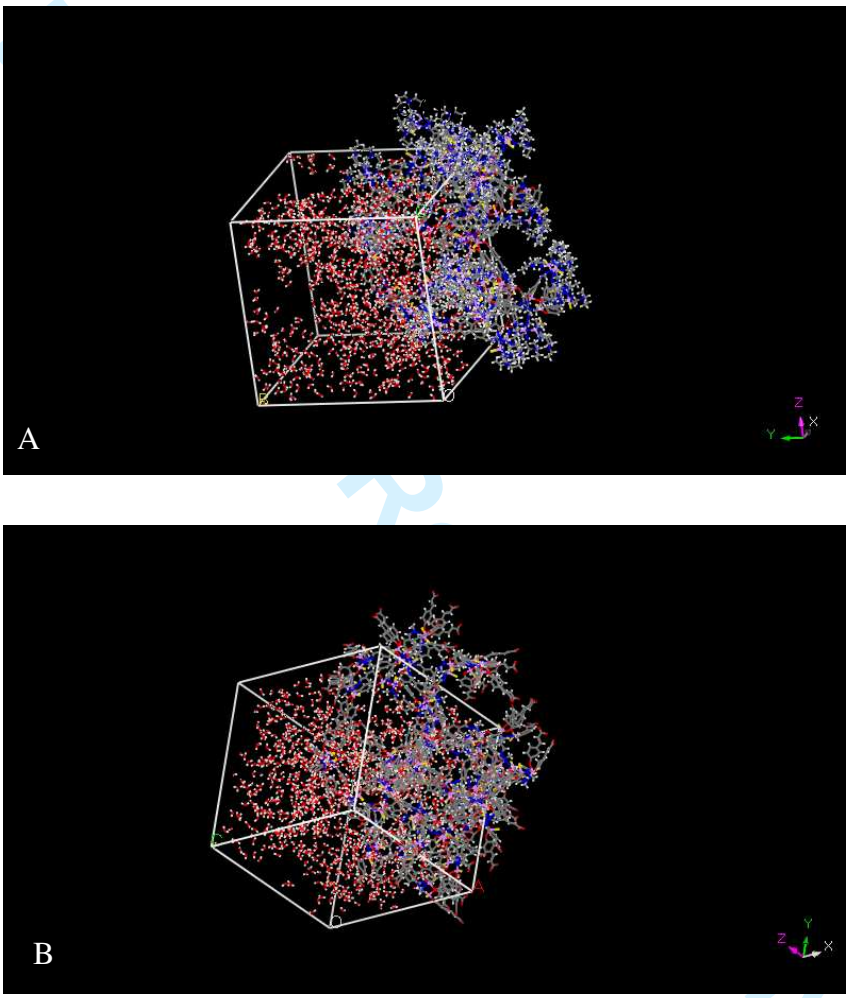

Figure (4): Amorphous cell of (A): G_4^+ and (B): G_4^- dendrimers in water

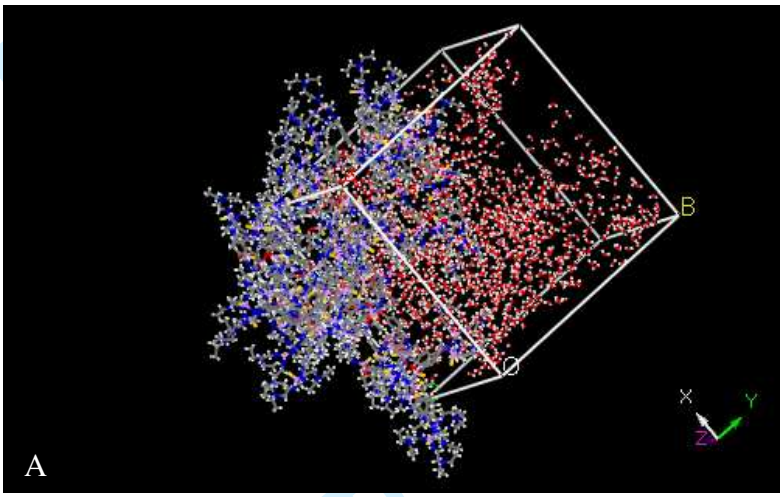

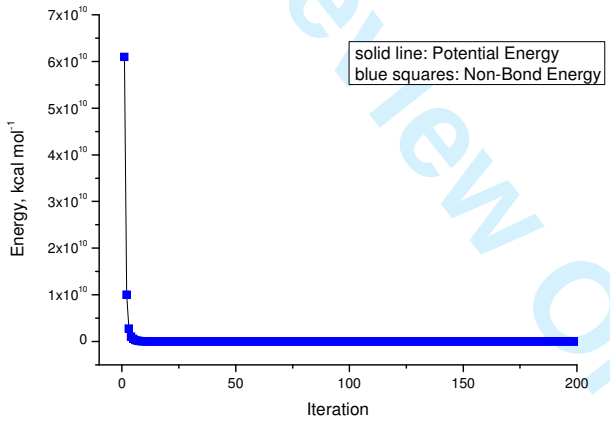

B

Figure (5): (A): Structure of G_4^+ after energy minimization; (B): Energy vs. number of iterations diagram showing the energy difference between the start and end structures.

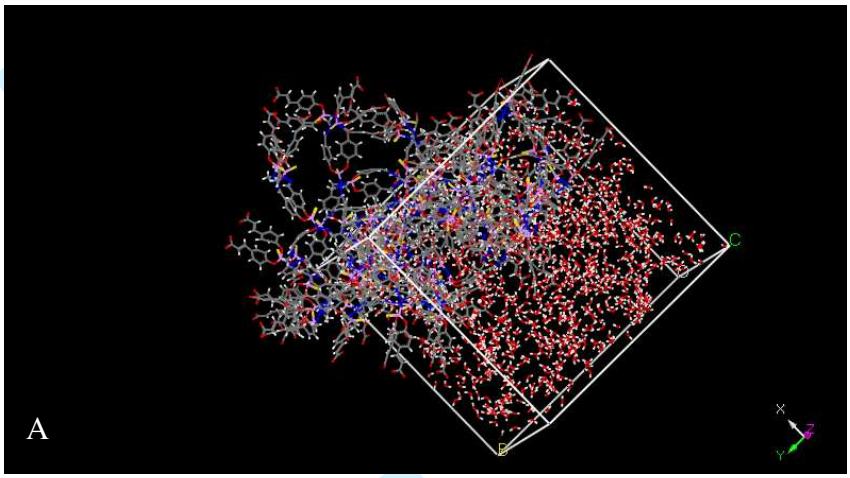

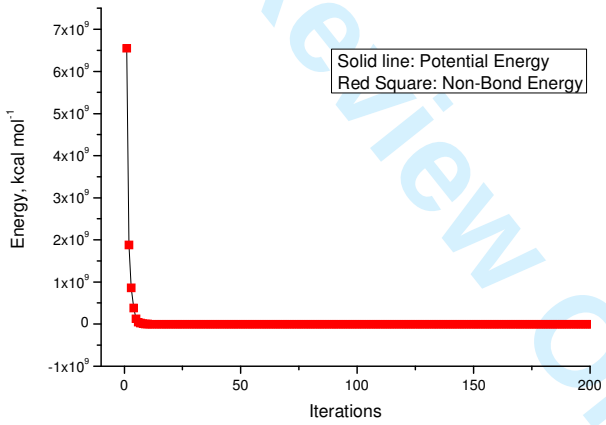

B

Figure (6): (A): Structure of G_4^- after energy minimization; (B): Energy vs. number of iterations diagram showing the energy difference between the start and end structures.